PDH activity was almost normal in *mpc1*Δ cells grown in rich medium [when the E2 subunit was lipoylated (Fig. 2C)]. Thus, the MPC proteins appeared to act upstream of PDH and may function in the transport of pyruvate into mitochondria. We therefore measured uptake of ^{14}C pyruvate in mitochondria isolated from WT, *mpc1*Δ, *mpc2*Δ, *mpc3*Δ, and *mpc2*Δ*mpc3*Δ cells grown in lactate medium (Fig. 3A). The specificity of uptake was assessed by the use of UK5099, an inhibitor of the mitochondrial pyruvate carrier (*14*). Uptake of pyruvate in WT mitochondria was sensitive to the proton ionophore carbonyl cyanide m-chloro phenyl hydrazone (CCCP) (Fig. 3B). Mitochondria from *mpc1*Δ and *mpc2*Δ*mpc3*Δ cells showed decreased pyruvate uptake (Fig. 3, A and B), despite a normal mitochondrial membrane potential (fig. S5). Surprisingly, deletion of *MPC3* alone impaired pyruvate uptake in mitochondria, whereas mitochondria from the *mpc2*Δ mutant transported pyruvate normally. Because this result did not correlate with the phenotypes of *mpc2*Δ and *mpc3*Δ single mutants grown in SD, we investigated the expression of Mpc2 and Mpc3 in SD and lactate media. In SD, yeast expressed mainly Mpc2, whereas in lactate medium, they mainly expressed Mpc3 (Fig. 3C). This expression pattern could be explained, at least in part, by the presence of binding sites for Gcn4 (a transcription factor activated by amino acid starvation) upstream of *MPC2* (*15*). This raises the possibility that under certain growth conditions, these two proteins might have specific, nonredundant functions.

We next assessed whether mouse MPC1 (mMPC1) and MPC2 (mMPC2) could restore growth of yeast cells lacking a functional pyruvate transporter (Fig. 4, A and B). mMPC1 alone restored growth of *mpc1*Δ cells, but mMPC2 failed to restore growth of the double-deletion strain of its orthologous genes *MPC2* and *MPC3*. However, growth of the triple-deletion strain *mpc1*Δ*mpc2*Δ*mpc3*Δ or of *mpc2*Δ*mpc3*Δ cells was restored by coexpression of both mMPC1 and mMPC2 (Fig. 4A). Thus, mMPC1 and mMPC2 together functionally complement the absence of pyruvate transport. We next expressed mMPC1 and mMPC2, alone and in combination, in the bacterium *Lactococcus lactis* (Fig. 4C), which has been successfully used to express and characterize mitochondrial transporters (*16*). No pyruvate uptake was observed in bacteria expressing either protein alone compared with the empty vector control. However, a fourfold increase in pyruvate uptake was detected when mMPC1 and mMPC2 were coexpressed (Fig. 4, D and E). This uptake was sensitive to the mitochondrial pyruvate carrier inhibitor UK5099 and to 2-deoxyglucose, which collapses the proton electrochemical gradient (Fig. 4E) (*17*). Moreover, artificially increasing the membrane potential by lowering the pH in the import buffer from 7.2 to 6.2 significantly increased pyruvate uptake (two-tailed *t* test, $P < 0.05$) (Fig. 4E). Thus, coexpression of mMPC1 and mMPC2 in bacteria is sufficient to allow import of pyruvate with similar properties to the mitochondrial pyruvate carrier (*3*). We therefore conclude that the mitochondrial pyruvate carrier is composed of Mpc1 and either Mpc2 or Mpc3 in yeast and of MPC1 and MPC2 in mammals.

References and Notes

1. J. K. Hiltunen, Z. Chen, A. M. Haapalainen, R. K. Wierenga, A. J. Kastaniotis, *Prog. Lipid Res.* **49**, 27 (2010).
2. L. J. Reed, *J. Biol. Chem.* **276**, 38329 (2001).
3. A. P. Halestrap, *Biochem. J.* **148**, 85 (1975).
4. S. Da Cruz *et al.*, *J. Biol. Chem.* **278**, 41566 (2003).
5. D. K. Bricker *et al.*, *Science* **337**, 96 (2012).
6. J. R. Dickinson, I. W. Dawes, *J. Gen. Microbiol.* **138**, 2029 (1992).
7. J. R. Dickinson, D. J. Roy, I. W. Dawes, *Mol. Gen. Genet.* **204**, 103 (1986).
8. R. A. Harris, M. Joshi, N. H. Jeoung, M. Obayashi, *J. Nutr.* **135** (suppl.), 1527S (2005).
9. M. S. Schonauer, A. J. Kastaniotis, V. A. Kursu, J. K. Hiltunen, C. L. Dieckmann, *J. Biol. Chem.* **284**, 23234 (2009).
10. J. E. Lawson, R. H. Behal, L. J. Reed, *Biochemistry* **30**, 2834 (1991).
11. K. M. Humphries, L. I. Szweda, *Biochemistry* **37**, 15835 (1998).
12. H. Wada, D. Shintani, J. Ohlrogge, *Proc. Natl. Acad. Sci. U.S.A.* **94**, 1591 (1997).
13. U. Hoja *et al.*, *J. Biol. Chem.* **279**, 21779 (2004).
14. A. P. Halestrap, R. M. Denton, *Biochem. J.* **148**, 97 (1975).
15. K. D. MacIsaac *et al.*, *BMC Bioinformatics* **7**, 113 (2006).
16. E. R. Kunji, D. J. Slotboom, B. Poolman, *Biochim. Biophys. Acta* **1610**, 97 (2003).
17. E. R. Kunji, E. J. Smid, R. Plapp, B. Poolman, W. N. Konings, *J. Bacteriol.* **175**, 2052 (1993).

Acknowledgments: We are grateful to R. Loewith and F. Stutz for strains and technical help, L. Szweda for antibodies, A. Kastaniotis for technical help on lipoic acid determination, Y. Que for erythromycin resistance cassette, and H. Riezman, A. Jourdain, and the Martinou lab for fruitful discussions. This work was supported by Novartis Science Foundation (S.H.), the Swiss National Science Foundation (subsidy 31003A-141068/1 to J.-C.M.), and the state of Geneva.

Supplementary Materials

www.sciencemag.org/cgi/content/full/science.1218530/DC1
Materials and Methods
Supplementary Text
Figs. S1 to S5
Table S1
References (*18*–*23*)

29 December 2011; accepted 11 May 2012
Published online 24 May 2012;
10.1126/science.1218530

A Mitochondrial Pyruvate Carrier Required for Pyruvate Uptake in Yeast, *Drosophila*, and Humans

Daniel K. Bricker,[1]* Eric B. Taylor,[2]* John C. Schell,[2]* Thomas Orsak,[2]* Audrey Boutron,[3] Yu-Chan Chen,[2] James E. Cox,[4] Caleb M. Cardon,[2] Jonathan G. Van Vranken,[2] Noah Dephoure,[5] Claire Redin,[6] Sihem Boudina,[7] Steven P. Gygi,[5] Michèle Brivet,[3] Carl S. Thummel,[1] Jared Rutter[2]†

Pyruvate constitutes a critical branch point in cellular carbon metabolism. We have identified two proteins, Mpc1 and Mpc2, as essential for mitochondrial pyruvate transport in yeast, *Drosophila*, and humans. Mpc1 and Mpc2 associate to form an ~150-kilodalton complex in the inner mitochondrial membrane. Yeast and *Drosophila* mutants lacking *MPC1* display impaired pyruvate metabolism, with an accumulation of upstream metabolites and a depletion of tricarboxylic acid cycle intermediates. Loss of yeast Mpc1 results in defective mitochondrial pyruvate uptake, and silencing of *MPC1* or *MPC2* in mammalian cells impairs pyruvate oxidation. A point mutation in *MPC1* provides resistance to a known inhibitor of the mitochondrial pyruvate carrier. Human genetic studies of three families with children suffering from lactic acidosis and hyperpyruvatemia revealed a causal locus that mapped to *MPC1*, changing single amino acids that are conserved throughout eukaryotes. These data demonstrate that Mpc1 and Mpc2 form an essential part of the mitochondrial pyruvate carrier.

Pyruvate occupies a pivotal node in the regulation of carbon metabolism as it is the end product of glycolysis and a major substrate for the tricarboxylic acid (TCA) cycle in mitochondria. Pyruvate lies at the intersection of these catabolic pathways with anabolic pathways for lipid synthesis, amino acid biosynthesis, and gluconeogenesis. As a result, the failure to correctly partition carbon between these fates lies at the heart of the altered metabolism evident in diabetes, obesity, and cancer (*1*, *2*). Owing to the fundamental importance of pyruvate, the mitochondrial pyruvate carrier (MPC) has been studied extensively (*3*, *4*). This included the discovery that α-cyanocinnamate analogs, such as UK-5099, act as specific and potent inhibitors of carrier activity (*5*). In spite of this characterization, however, the gene or genes that encode the mitochondrial pyruvate carrier remain unknown (*6*, *7*).

As part of an ongoing effort to characterize mitochondrial proteins that are conserved through evolution, we initiated studies of the MPC protein family (originally designated BRP44 and BRP44L

in humans) (*8*). This family contains three members in *Saccharomyces cerevisiae*, encoded by *YGL080W*, *YHR162W*, and *YGR243W*, hereafter referred to as *MPC1*, *MPC2*, and *MPC3*, respectively. Mpc2 and Mpc3 are 79% identical in amino acid sequence and appear to be the product of a recent gene duplication event. Mpc1, Mpc2, and Mpc3 colocalize with mitochondria (Fig. 1A and fig. S2A), consistent with published mitochondrial proteomic studies (*9*, *10*). The mitochondrial localization of Mpc1 and Mpc2 was confirmed by biochemical fractionation (Fig. 1B). Mpc1, Mpc2, and Mpc3 were enriched in mitochondrial membranes (fig. S2B), consistent with the presence of predicted transmembrane domains in their sequences (fig. S1). Mpc1 and Mpc2 were resistant to protease treatment unless the mitochondrial outer membrane was ruptured (Fig. 1B and fig. S2C), implying that they are embedded in the mitochondrial inner membrane. Chromatographic purification of tagged variants of Mpc1 and Mpc2, followed by mass spectrometry, revealed that Mpc2 and Mpc3 were among the major interacting proteins of Mpc1, and Mpc1 and Mpc3 were among the major interacting proteins of Mpc2 (table S1). Consistent with this, immunoprecipitation of tagged Mpc1 copurified Mpc2 and vice versa (Fig. 1C, lanes 3 and 4). In addition, Mpc2 can interact with itself (Fig. 1C, lane 8), whereas an Mpc1 homotypic interaction was not detected (Fig. 1C, lane 7). Blue native–polyacrylamide gel electrophoresis showed that both Mpc1 and Mpc2 migrated as part of an ~150-kD complex (fig. S2D). Loss of Mpc2 prevented Mpc1 from migrating in this complex, whereas an *mpc1*Δ strain showed elevated Mpc2 complex formation (fig. S2E). We conclude that Mpc1 and Mpc2 form a multimeric complex embedded in the mitochondrial inner membrane, with Mpc2 likely being the major structural subunit.

Mutant yeast strains were subjected to a variety of growth conditions. The *mpc1*Δ and *mpc2*Δ cells displayed mild growth defects on nonfermentable carbon sources like glycerol, with greater effects on glucose medium (fig. S3) and a strong growth defect in the absence of leucine (Fig. 1D). In contrast, *mpc3*Δ mutant displayed no apparent growth phenotypes. Yeast, *Drosophila*, or human *MPC1* orthologs, but not human *MPC2*, could rescue the *mpc1*Δ growth phenotype (Fig. 1E), indicating that Mpc1 function is conserved through evolution.

To analyze the physiological function of MPCs in a multicellular animal, we extended our studies to the *Drosophila* ortholog of MPC1 (dMPC1; encoded by *CG14290*), which also localized to mitochondria (fig. S4). Analogous to yeast *mpc1*Δ mutants, *dMPC1* mutants (fig. S5) were viable on standard food, but sensitive to a carbohydrate-only diet, with rapid lethality after transfer to a sucrose medium (Fig. 2A). Whereas the amount of adenosine 5′-triphosphate (ATP) was reduced in *dMPC1* mutants (Fig. 2C), along with triacylglycerol (TAG) and protein (fig. S6, B and C), the amounts of carbohydrates were elevated, including the circulating sugar trehalose (Fig. 2D), glucose (Fig. 2E), fructose, and glycogen (fig. S6, A and D). These results suggest that *dMPC1* mutants are defective in carbohydrate metabolism and may consume stored fat and protein for energy. Consistent with this, the lethality of *dMPC1* mutants on the sugar diet was rescued by expression of the wild-type gene in tissues that depend heavily on glucose metabolism: the fat body, muscle, and neurons (Fig. 2B).

Metabolomic analyses revealed that the concentration of pyruvate was highly elevated, whereas TCA cycle intermediates were significantly

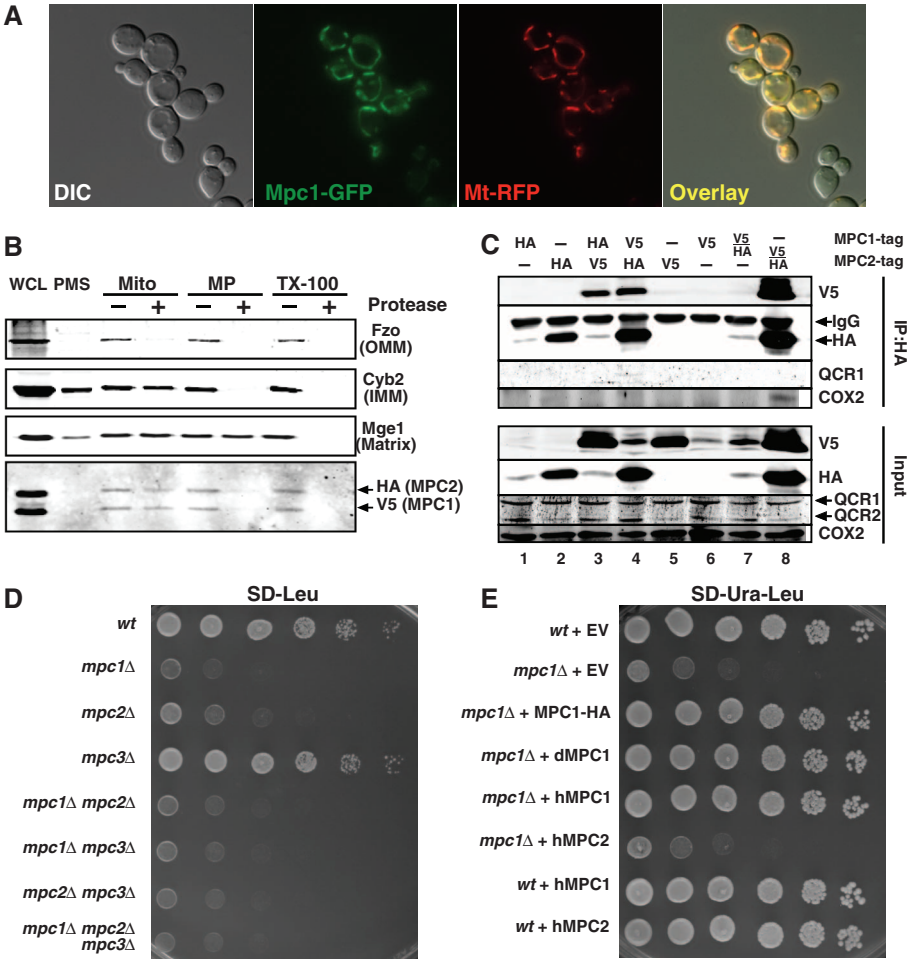

Fig. 1. Mpc1 and Mpc2 are evolutionarily conserved mitochondrial inner-membrane proteins. (**A**) Mpc1 labeled with green fluorescent protein (Mpc1-GFP) and mitochondrial targeted red fluorescent protein (MtRFP) coexpressed in yeast cells. DIC, differential interference contrast. (**B**) Intact mitochondria, hypotonic-swollen mitoplasts, and TritonX-100–solubilized mitochondria from a strain expressing Mpc1-V5 and Mpc2-His_6/HA_2 with (+) or without (–) proteinase K incubation. An immunoblot of extracts using the indicated antibodies with the whole-cell lysate (WCL) and postmitochondrial supernatant (PMS) is shown. Mge1, Cyb2, and Fzo1 are matrix, intermembrane space, and outer-membrane proteins, respectively. (**C**) Immunoprecipitations from mitochondrial extracts from *mpc1*Δ *mpc2*Δ cells expressing Mpc1 and Mpc2 tagged as indicated. Immunoblot of either immunoprecipitate (IP:HA) or input is shown (HA, hemagglutinin). QCR1 and 2 (ubiquinol–cytochrome c reductase complex core protein 1 and 2) along with Cox II (cytochrome c oxidase subunit 2) are controls for the specificity of the immunoprecipitation. (**D**) Serial dilutions of the indicated yeast strains spotted on synthetic media lacking leucine and grown at 30°C for 24 hours. (**E**) Serial dilutions of indicated strains spotted on synthetic media lacking leucine and grown at 30°C for 48 hours. *wt*, wild type; EV, empty vector.

[1]Department of Human Genetics, University of Utah School of Medicine, Salt Lake City, UT 84112, USA. [2]Department of Biochemistry, University of Utah School of Medicine, Salt Lake City, UT 84112, USA. [3]Laboratoire de Biochimie, AP-HP Hôpital de Bicêtre, Le Kremlin Bicêtre, France. [4]Metabolomics Core Research Facility, University of Utah School of Medicine, Salt Lake City, UT 84112, USA. [5]Department of Cell Biology, Harvard Medical School, Boston, MA 02115, USA. [6]Institut de Genetique et de Biologie Moleculaire et Cellulaire (IGBMC), Strasbourg, France. [7]Department of Medicine, University of Utah School of Medicine, Salt Lake City, UT 84112, USA.

*These authors contributed equally to this work.
†To whom correspondence should be addressed. E-mail: rutter@biochem.utah.edu

depleted in *dMPC1* mutants on the sugar diet (Fig. 2F). Similarly, the amounts of glycine and serine, which can interconvert with glycolytic intermediates, were elevated in the mutants on the sugar diet (fig. S6E), whereas glutamate, aspartate, and proline, which can interconvert with TCA cycle intermediates, were depleted under these conditions (fig. S6F). Consistent with this, metabolomic analysis of *mpc1*Δ and *mpc2*Δ yeast mutants revealed elevated pyruvate concentrations (Fig. 3A), depletion of malate (fig. S7), depleted acetyl–coenzyme A (CoA), and elevated CoA concentrations (Fig. 3B). Taken together, these results suggest that *MPC1* mutants are unable to efficiently convert cytosolic pyruvate to mitochondrial acetyl-CoA to drive the TCA cycle and ATP production.

These phenotypes could arise from either a defect in mitochondrial pyruvate uptake or the conversion of mitochondrial pyruvate into acetyl-CoA by the pyruvate dehydrogenase (PDH) complex. Yeast lacking Mpc1, however, had nearly wild-type PDH activity, unlike the strong decrease seen in *pda1*Δ mutants (Fig. 3C), which lack PDH function (*11*). A decrease in PDH activity also does not explain the growth defect of *mpc1*Δ mutants, which is more severe than that of the *pda1*Δ mutant (fig. S8). However, combining the *mpc1*Δ allele with a deletion for *mae1*, which encodes a malic enzyme that converts malate to pyruvate in the mitochondrial matrix (*12*), revealed a profound growth defect on glucose medium that was completely rescued by plasmid expression of either *MAE1* or *MPC1* (Fig. 3D). Notably, mitochondria from the *mpc1*Δ mutant displayed almost no uptake of ^{14}C-pyruvate, which could be fully rescued by plasmid expression of wild-type *MPC1* (Fig. 3E). Moreover, Mpc1 appears to be a key target for UK-5099, which is an inhibitor of the mitochondrial pyruvate carrier (*5*). The *mae1*Δ *mpc1*Δ double mutant displayed reduced growth on glucose medium lacking leucine, and this phenotype could be effectively rescued by transgenic expression of wild-type *MPC1* in the absence, but not the presence, of UK-5099 (Fig. 3F). By screening for *MPC1* mutants that could grow in the presence of UK-5099, we recovered an Asp^{118}→Gly (D118G) substitution in Mpc1 that conferred UK-5099 resistance (Fig. 3F). Moreover, whereas ^{14}C-pyruvate uptake into mitochondria expressing wild-type *MPC1* was almost completely inhibited by UK-5099, efficient pyruvate uptake that is resistant to UK-5099 was recovered upon expression of *MPC1-D118G* (Fig. 3G). We conclude that Mpc1 is a key component of the mitochondrial pyruvate carrier that corresponds to the activity studied for decades by Halestrap and others (*5*, *13*).

Depletion of *MPC1* in mouse embryonic fibroblasts (fig. S9A) caused a modest decrease in pyruvate-driven oxygen consumption under basal conditions, and a stronger reduction in the presence of carbonyl cyanide-*p*-trifluoromethoxyphenylhydrazone (FCCP), which stimulates maximal respiration (Fig. 4A). Similar results were also seen upon silencing *MPC2* (Fig. 4B and fig. S9A). This suppression of pyruvate oxidation, which occurred without affecting components of the oxidative phosphorylation machinery (fig. S9, B and C), suggests that mammalian Mpc1 and Mpc2 mediate mitochondrial pyruvate uptake in a manner similar to that seen in yeast and *Drosophila*.

We have previously described a French-Algerian family with two offspring that exhibited a devastating defect in mitochondrial pyruvate oxidation (*14*) (Fig. 4C, family 1). We subsequently discovered two additional families, each with one affected child who displayed a similar, but less severe, phenotype (Fig. 4C, families 2 and 3). Linkage analysis and homozygosity mapping allowed us to focus on one candidate region on chromosome 6 (163,607,637 to 166,842,083, GRCh37/hg19). This interval contained 10 potential candidate genes: *PACRG*, *QKI*, *C6orf118*, *PDE10A*, *SDIM1*, *T*, *PRR18*, *SFT2D1*, *RPS6KA2*, and *BRP44L*, which is the human *MPC1*. DNA sequencing of the exons and intron/exon boundaries of the *MPC1* gene in fibroblasts from the affected patients in families 2 and 3 revealed the same molecular lesion, c.236T→A, causing a predicted p.Leu^{79}→His (L79H) alteration (Fig. 4D). Analysis of DNA from family 1 revealed a distinct sequence change, c.289C→T, which resulted in a predicted p.Arg^{97}→Trp (R97W) mutation (Fig. 4D). Both of the affected residues are conserved through evolution between *MPC1* orthologs, and Arg^{97} is conserved among both *MPC1* and *MPC2* orthologs (fig. S1).

Cells from the affected individuals in families 1 and 2 exhibited impaired basal and FCCP-stimulated pyruvate oxidation (Fig. 4E), whereas glutamine-driven oxygen consumption was normal or elevated, demonstrating that they have not acquired a generalized impairment of mitochondrial respiration (Fig. 4E). As expected, expression of wild-type human *MPC1* in the cells from family 2 (Fig. 4F) or family 1 (Fig. 4G) either completely or partially rescued the defect in FCCP-induced pyruvate oxidation. Moreover, expression of the *MPC1-Leu79His* allele was less effective at suppressing the yeast *mpc1*Δ growth defect relative to wild-type human *MPC1* (Fig. 4H), and the stronger *MPC1-Arg97Trp* allele was

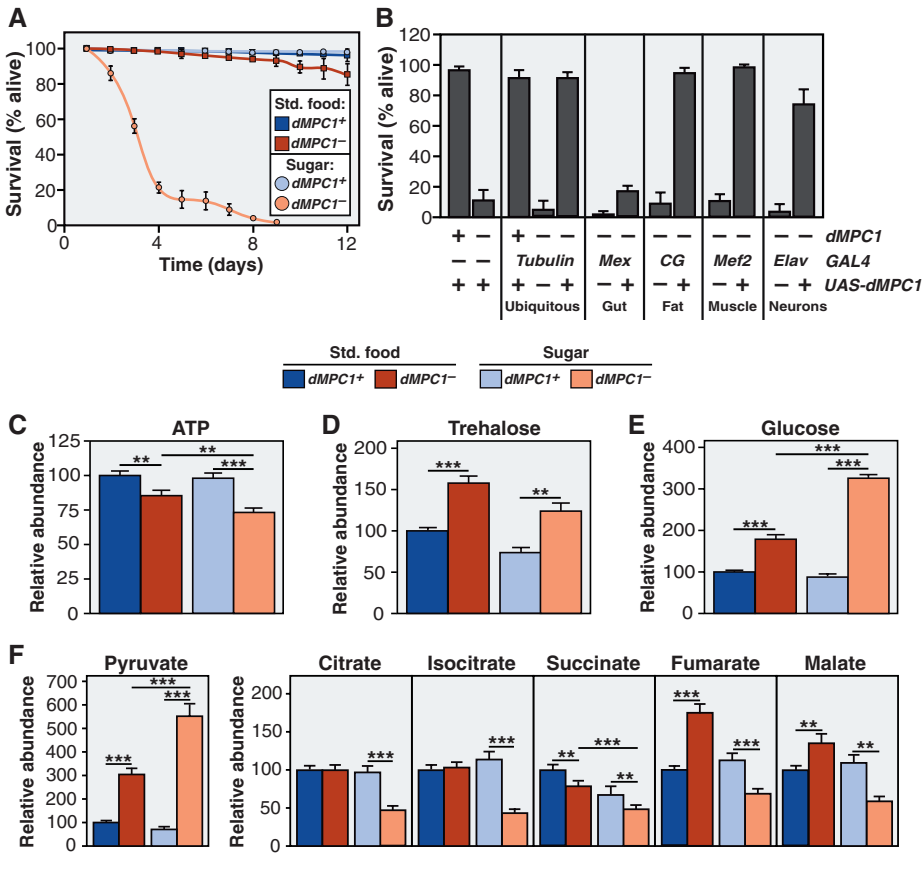

Fig. 2. *dMPC1* is required for pyruvate metabolism in *Drosophila*. (**A**) Percentage of living control (*dMPC1*$^+$) or *dMPC1* mutant (*dMPC*$^-$) flies after transfer to standard laboratory medium (std. food) or to media containing only sugar. (**B**) Percentage of living *dMPC1*$^+$ or *dMPC*$^-$ flies carrying the indicated GAL4 and UAS transgenes on sugar media after 8 days. (**C** to **E**) Relative concentration of ATP (C), trehalose (D), and glucose (E) in extracts from *dMPC1*$^+$ or *dMPC*$^-$ flies on the indicated diet after either 2 days (D and E) or 3 days (C). (**F**) Relative abundance of pyruvate and TCA cycle intermediates in *dMPC1*$^+$ or *dMPC*$^-$ flies after 2 days on the indicated diet as measured by gas chromatography–mass spectrometry. *$P < 0.05$, **$P < 0.01$, and ***$P < 0.001$ (Student's *t* test). Data are shown as mean ± SEM.

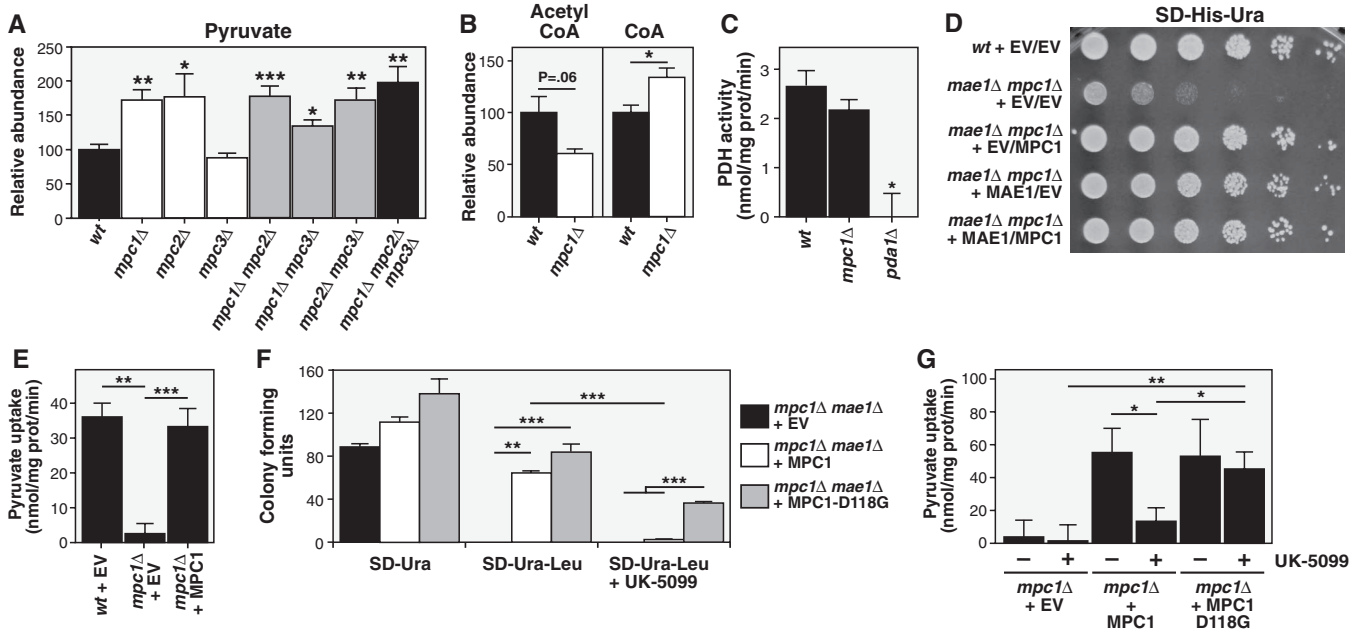

Fig. 3. *MPC1* is required for mitochondrial pyruvate uptake. (**A**) Relative abundance of pyruvate in the indicated strains. *P* values relative to *wt*. (**B**) Relative abundance of acetyl-CoA and CoA in the indicated strains. (**C**) Mitochondrial pyruvate dehydrogenase activity in the indicated strains. *P* value relative to *wt* and *mpc1*Δ. (**D**) Serial dilutions of the indicated strain on glucose medium grown at 30°C for 48 hours. (**E**) Uptake of ^{14}C-pyruvate into mitochondria purified from either *wt* or *mpc1*Δ cells containing the indicated plasmid. *P* value relative to *wt* + *EV* and *mpc1*Δ + *MPC1*. (**F**) *Mae1*Δ *mpc1*Δ cells transformed with the indicated plasmid and plated on media containing or lacking combinations of leucine or UK-5099. (**G**) Uptake of ^{14}C-pyruvate into mitochondria isolated from the *mpc1*Δ strain containing the indicated plasmid in the presence or absence of UK-5099. ***$P < 0.001$, **$P < 0.01$, *$P < 0.05$; NS, not significant (Student's *t* test). Data are shown as mean ± SEM.

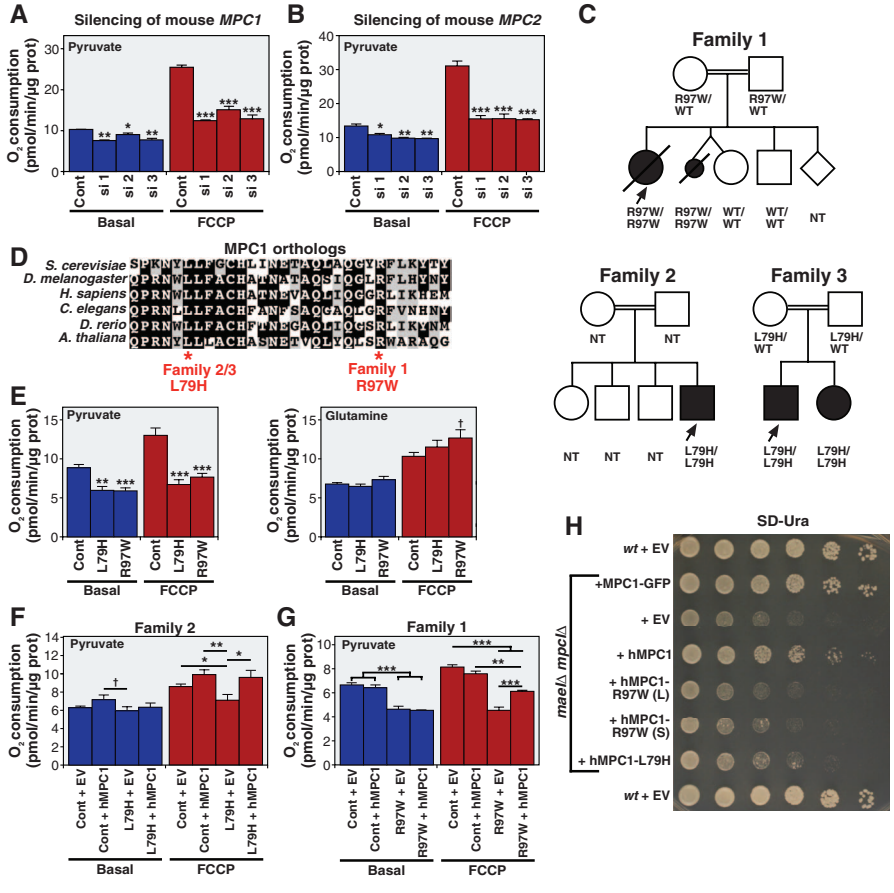

Fig. 4. Mammalian *MPC1* and *MPC2* are required for normal pyruvate metabolism. (**A** and **B**) Pyruvate-driven respiration in mouse embryonic fibroblasts under basal and FCCP-stimulated conditions in cells transfected with either control (Cont) small interfering RNAs (siRNAs) or three different siRNAs (si 1–3) targeted to either *MPC1* (A) or *MPC2* (B). *P* values relative to control. (**C**) Pedigrees of families 1, 2, and 3. Circles indicate females; squares, males; and diamonds, unknown sex. Black indicates deceased and white, living. Arrows mark individuals from whom fibroblasts were obtained. (**D**) The protein region of MPC1 containing the predicted amino acid substitutions from all three families aligned by ClustalW. Single-letter abbreviations for the amino acid residues are as follows: A, Ala; C, Cys; D, Asp; E, Glu; F, Phe; G, Gly; H, His; I, Ile; K, Lys; L, Leu; M, Met; N, Asn; P, Pro; Q, Gln; R, Arg; S, Ser; T, Thr; V, Val; W, Trp; and Y, Tyr. *Saccharomyces cerevisiae, Drosophila melanogaster, Homo sapiens, Caenorhabditis elegans, Danio rerio, Arabidopsis thaliana*. (**E**) Pyruvate- (left) and glutamine- (right) supported respiration of fibroblasts harboring either L79H or R97W *MPC1* mutations. (**F**) Pyruvate-supported respiration of either a control or an L79H patient cell line after transduction with the indicated vector. (**G**) Pyruvate-supported respiration of either a control or an R97W patient cell line after transduction with the indicated vector. (**H**) Serial dilutions of *wt* or *mae1*Δ *mpc1*Δ yeast strains carrying the indicated plasmid grown on medium lacking uracil for plasmid selection at 30°C for 40 hours. Both long (L) and short (S) forms of R97W were used (with or without exon 4). ***$P < 0.001$, **$P < 0.01$, *$P < 0.05$, $^{\dagger}P < 0.10$; NS, not significant (Student's *t* test). Data are shown as mean ± SEM.

essentially inactive (Fig. 4H), suggesting that *MPC1* function is evolutionarily conserved from yeast to humans.

The data presented here demonstrate that the Mpc1-Mpc2 complex is an essential component of the mitochondrial pyruvate carrier in yeast, flies, and mammals. This is consistent with experiments performed in rat liver, heart, and castor beans, which implicated proteins of 12 to 15 kD in mitochondrial pyruvate uptake (*15*)—similar to the molecular masses of Mpc1 (15 kD), Mpc2 (14 kD), and Mpc3 (16 kD). Although these individual sizes are relatively small, Mpc1 and Mpc2 form a complex of ~150 kD, suggesting that an oligomeric structure mediates pyruvate transport. The demonstration that Mpc1 and Mpc2 are sufficient to promote pyruvate uptake in a heterologous system provides further evidence that they constitute an essential pyruvate transporter (*16*). Finally, the degree to which carbohydrates are imported into mitochondria and converted into acetyl-CoA is a critical step in normal glucose oxidation as well as the onset of diabetes, obesity, and cancer. Thus, like PDH, which is controlled by allostery and posttranslational modification (*17*), the mitochondrial import of pyruvate is likely to be precisely regulated (*18*, *19*). The identification of Mpc1 and Mpc2 as critical for mitochondrial pyruvate transport provides a new framework for understanding this level of metabolic control, as well as new directions for potential therapeutic intervention.

References and Notes

1. D. Hanahan, R. A. Weinberg, *Cell* **144**, 646 (2011).
2. S. E. Kahn, R. L. Hull, K. M. Utzschneider, *Nature* **444**, 840 (2006).
3. A. P. Halestrap, R. M. Denton, *Biochem. J.* **138**, 313 (1974).
4. A. P. Halestrap, *Biochem. J.* **172**, 377 (1978).
5. A. P. Halestrap, *Biochem. J.* **148**, 85 (1975).
6. S. Todisco, G. Agrimi, A. Castegna, F. Palmieri, *J. Biol. Chem.* **281**, 1524 (2006).
7. J. C. Hildyard, A. P. Halestrap, *Biochem. J.* **374**, 607 (2003).
8. M. Jiang *et al.*, *Mol. Biol. Rep.* **36**, 215 (2009).
9. D. J. Pagliarini *et al.*, *Cell* **134**, 112 (2008).
10. A. Sickmann *et al.*, *Proc. Natl. Acad. Sci. U.S.A.* **100**, 13207 (2003).
11. H. Y. Steensma, L. Holterman, I. Dekker, C. A. van Sluis, T. J. Wenzel, *Eur. J. Biochem.* **191**, 769 (1990).
12. E. Boles, P. de Jong-Gubbels, J. T. Pronk, *J. Bacteriol.* **180**, 2875 (1998).
13. S. Papa, G. Paradies, *Eur. J. Biochem.* **49**, 265 (1974).
14. M. Brivet *et al.*, *Mol. Genet. Metab.* **78**, 186 (2003).
15. A. P. Thomas, A. P. Halestrap, *Biochem. J.* **196**, 471 (1981).
16. S. Herzig *et al.*, *Science* **337**, 93 (2012).
17. R. A. Harris, M. M. Bowker-Kinley, B. Huang, P. Wu, *Adv. Enzyme Regul.* **42**, 249 (2002).
18. F. M. Zwiebel, U. Schwabe, M. S. Olson, R. Scholz, *Biochemistry* **21**, 346 (1982).
19. R. Rognstad, *Int. J. Biochem.* **15**, 1417 (1983).
20. Materials and methods are available as supplementary materials on *Science* Online.

Acknowledgments: We thank members of the Rutter, Thummel, Winge, Stillman, Shaw, and Metzstein laboratories for helpful discussions. We thank the Shaw and Winge labs for the antibodies against Fzo1, Cyb2, and Mge1 and for the mito-RFP constructs. We thank J. M. Saudubray, L. Burglen, and H. Tevissen for referring patients and C. Thibault and J. L. Mandel (IGBMC, Strasbourg, France) for assistance in single-nucleotide polymorphism array hybridization. This research was supported by NIH grants R01GM083746 (J.R.), RC1DK086426 (C.S.T.), and R24DK092784 (J.R. and C.S.T.) and a pilot grant from P30DK072437 (J.R.). D.K.B. and C.M.C. were supported by the NIH Genetics Predoctoral Training Grant T32GM007464. E.B.T. was supported by NIH Pathway to Independence award K99AR059190. D.K.B., T.O., C.S.T., and J.R. are inventors on a patent application by the University of Utah covering the discovery of the MPC complex.

Supplementary Materials

www.sciencemag.org/cgi/content/full/science.1218099/DC1
Materials and Methods
Figs. S1 to S10
Table S1
References

19 December 2011; accepted 9 May 2012
Published online 24 May 2012;
10.1126/science.1218099

An Abundance of Rare Functional Variants in 202 Drug Target Genes Sequenced in 14,002 People

Matthew R. Nelson,[1]*† Daniel Wegmann,[2]* Margaret G. Ehm,[1] Darren Kessner,[2] Pamela St. Jean,[1] Claudio Verzilli,[3] Judong Shen,[1] Zhengzheng Tang,[4] Silviu-Alin Bacanu,[1] Dana Fraser,[1] Liling Warren,[1] Jennifer Aponte,[1] Matthew Zawistowski,[5] Xiao Liu,[6] Hao Zhang,[6] Yong Zhang,[6] Jun Li,[7] Yun Li,[4] Li Li,[1] Peter Woollard,[3] Simon Topp,[3] Matthew D. Hall,[3] Keith Nangle,[1] Jun Wang,[6,8] Gonçalo Abecasis,[5] Lon R. Cardon,[9] Sebastian Zöllner,[5,10] John C. Whittaker,[3] Stephanie L. Chissoe,[1] John Novembre,[2]†‡ Vincent Mooser[9]‡

Rare genetic variants contribute to complex disease risk; however, the abundance of rare variants in human populations remains unknown. We explored this spectrum of variation by sequencing 202 genes encoding drug targets in 14,002 individuals. We find rare variants are abundant (1 every 17 bases) and geographically localized, so that even with large sample sizes, rare variant catalogs will be largely incomplete. We used the observed patterns of variation to estimate population growth parameters, the proportion of variants in a given frequency class that are putatively deleterious, and mutation rates for each gene. We conclude that because of rapid population growth and weak purifying selection, human populations harbor an abundance of rare variants, many of which are deleterious and have relevance to understanding disease risk.

Understanding the genetic contribution to human disease requires knowledge of the abundance and distribution of functional genetic diversity within and among populations. The "common-disease rare-variant" hypothesis posits that variants affecting health are under purifying selection and thus should be found only at low frequencies in human populations (*1*–*3*). This hypothesis has become increasingly credible because very large genome-wide association studies of common variants have explained only a fraction of the known heritability of most traits (*4*, *5*). Investigating the role of rare variants for complex trait mapping has led to tests that aggregate rare variants (*6*) and determine the abundance, distribution, and phenotypic effects of rare variants in human populations (*7*, *8*).

Population genetic models predict that mutation rates, the strength of selection, and demography affect the abundance of rare variants, although the relative importance of each is a long-standing question (*9*–*11*). To understand rare variant diversity in humans, we sequenced 202 genes in a sample of 14,002 well-phenotyped individuals (table S1). These genes represent approximately 1% of the coding genome and approximately 7% of genes considered current or potential drug targets (*12*) and are enriched for cell-signaling proteins and membrane-bound transporters (table S2). A total of 864 kb were targeted, including 351 kb of coding and 323 kb of untranslated (UTR) exon regions (database S1). More than 93% of target bases were successfully

[1]Department of Quantitative Sciences, GlaxoSmithKline (GSK), Research Triangle Park, NC 27709, USA. [2]Department of Ecology and Evolutionary Biology, University of California–Los Angeles, Los Angeles, CA 90095, USA. [3]Department of Quantitative Sciences, GSK, Stevenage SG1 2NY, UK. [4]Department of Genetics and Biostatistics, University of North Carolina–Chapel Hill, Chapel Hill, NC 27599, USA. [5]Department of Biostatistics, University of Michigan–Ann Arbor, Ann Arbor, MI 48109, USA. [6]BGI, Shenzhen 518083, China. [7]Department of Human Genetics, University of Michigan–Ann Arbor, Ann Arbor, MI 48109, USA. [8]Department of Biology, Novo Nordisk Foundation Center for Basic Metabolic Research, University of Copenhagen, Copenhagen 3393 9524, Denmark. [9]Department of Quantitative Sciences, GSK, Upper Merion, PA 19406, USA. [10]Department of Psychiatry, University of Michigan–Ann Arbor, Ann Arbor, MI 48109, USA.

*These authors contributed equally to this work.
†To whom correspondence should be addressed. E-mail: matthew.r.nelson@gsk.com (M.R.N); jnovembre@ucla.edu (J.N.)
‡These authors contributed equally to this work.